Structure of Relativistic Magnetosonic Shocks in Electron-Positron Plasmas

A. Bruce Langdon, Jonathan Arons,[a] and Claire E. Max

Institute of Geophysics and Planetary Physics and Physics Department, Lawrence Livermore National Laboratory, University of California, Livermore, California 94550

(Received 4 March 1988)

The one-dimensional structure of high-Mach-number, transverse magnetosonic, relativistic shocks is studied computationally by kinetic, particle-in-cell methods. For amplitudes of astrophysical interest, shocks are mediated by magnetic reflection of the incoming plasma stream. The resulting coherent Larmor loops at the shock front are unstable, and rapidly thermalize downstream to form a relativistic, quasi-Maxwellian plasma in the momenta normal to the background magnetic field.

PACS numbers: 95.30.Qd, 52.35.Tc, 52.60.+h, 52.65.+z

Magnetized, electron-positron plasmas are thought to be the dominant constituent in the magnetospheres of rotation-powered pulsars.[1] Relativistic outflow of these plasmas[2,3] may be the energy source for the filled supernova remnants[4] surrounding active pulsars, of which the Crab nebula is the most prominent example. Similar plasmas may be the major material component in jets emanating from galactic nuclei[5] and in compact cores of these galaxies.[6] Nebulas driven by pulsars and extragalactic jets shine by synchrotron radiation. The energy for the accelerated, synchrotron-emitting particles is thought to come from the kinetic energy and Poynting flux of relativistic flows emanating from the energizing compact objects.[2,3,7] Shock waves in these relativistic flows are the most plausible candidate for conversion of flow energy into random energy of the synchrotron-emitting particles.[8-10] These shock waves are expected to be collisionless.

Relativistic shocks cannot be studied experimentally either in the laboratory or in interplanetary space. Theoretical studies of relativistic, magnetosonic solitary waves suggest that associated shocks have multistreaming components in the flow direction.[11] Kinetic computer simulations therefore provide the major means of investigating the nonlinear state of the plasma in these shocks. We present here the first particle-in-cell simulations of relativistic shock waves in an electron-positron plasma. Shock dissipation is due to collisionless effects; no model of collisional dissipation is added. Motivated by the applications to pulsar-driven nebulae,[2-4] and to termination shocks in extragalactic radio jets,[12] we examine shock structures with the upstream magnetic field polarized perpendicular to the flow direction.

The equations of motion and the Maxwell equations can be scaled[11] to parametrize soliton and shock structures solely by the ratio of the upstream Poynting flux to the upstream flux, $\sigma = B_\infty^2/8\pi N_\infty mc^2\gamma_\infty$. Here, $N_\infty = \gamma_\infty n_\infty$ is the upstream density of electrons or positrons measured in the frame where the fluid velocity is $c\beta_\infty$, n_∞ is the density in the proper frame, m is the rest mass of the particles, and the upstream Lorentz factor is $\gamma_\infty = (1-\beta_\infty^2)^{-1/2}$. Since the electric field $\mathbf{E}_\infty$ in the uniform flow upstream of the shock satisfies $\mathbf{E}_\infty + \beta_\infty \times \mathbf{B}_\infty = \mathbf{0}$, the magnetic field in the proper frame of the upstream fluid is B_∞/γ_∞. Using these relations and the Lorentz transformations of $\mathbf{B}_\infty$, γ_∞, and N_∞, one can show that σ is a Lorentz invariant with respect to transformations perpendicular to $\mathbf{B}_\infty$. The magnetosonic Mach number M_A is related to σ by $M_A^2 = (u'_\infty)^2/\sigma$, where $u'_\infty = \gamma_s u_\infty(1-\beta_s\beta_\infty)$ is the upstream momentum in the shock frame, in units of mc, $\beta_s = v_s/c$ is the (signed) shock velocity, and $\gamma_s = (1-\beta_s^2)^{-1/2}$. The ratio of the plasma frequency $\omega_{p\infty} \equiv (4\pi e^2 n_\infty/m)^{1/2}$ to the cyclotron frequency $\omega_{c\infty} \equiv eB_\infty/mc\gamma_\infty$ in the proper frame of the upstream flow is $\omega_{p\infty}/\omega_{c\infty} = \sigma^{-1/2}$. Our simulations are parametrized by σ.

Studies of magnetosonic solitary waves *without* reflected particles[13] suggest that shock compressions $r = B_{\text{downstream}}/B_\infty$ are limited to $r < 1 + 2/\gamma'_\infty$, corresponding to $M_A < M_1 = [2(\gamma'_\infty + 1)]^{1/2}$. This is equivalent to $\sigma > \sigma_1 \equiv (\gamma'_\infty - 1)/2$, corresponding to highly magnetized flow when $\gamma'_\infty \gg 1$. Astrophysically interesting amplitudes occur at smaller σ and larger M_A. Incorporation of magnetically reflected particles as a single Larmor loop[11] yields larger-amplitude solitons, with the peak amplitude limited to $B_{\max}/B_\infty \le \sqrt{11}$. These single-loop structures exist for $\sigma > 0.2$, $M_A < \sqrt{5}\gamma'_\infty$, suggesting that the associated shock waves will also show coherent Larmor-loop structure when $\sigma_1 > \sigma > 0.2$. Less electromagnetically dominated flows should show a more chaotic structure.

Our simulations used the electromagnetic particle-in-cell code ZOHAR,[14,15] in a single spatial dimension. All velocity and field components are included in the calculation, but in our transverse geometry, velocities in the plane perpendicular to the background magnetic field are uncoupled from motions parallel to $\mathbf{B}$. Particle motions, currents, and the electric field are all perpendicular to $\mathbf{B}$, while the induced magnetic field is parallel to the uniform magnetic field applied upstream.

The simulations are initialized by injection of a uniform upstream plasma from the left which travels toward

positive x with speed v_∞. At the injection boundary $x=0$, the plasma carries a uniform magnetic field B_∞. In order to minimize transients, the initial field was assumed to be uniform on the left two-thirds of the grid, and then was allowed to drop linearly to zero in the remaining one-third of the box. The properties of the incoming stream and its embedded magnetic field at $x=0$ are held fixed throughout the calculation. Particles which would cross the downstream boundary at $x=L_x$ during the time interval (t_n,t_{n+1}) are removed from the system if they do not bounce off a hypothetical moving elastic wall located at $L_w=L_x+\beta_w(t-t_n)$, or if they reflect from the wall but have positions $x_{n+1}>L_x$ at time t_{n+1}. It can be shown that this procedure forces the bulk flow speed of the plasma to be equal to $c\beta_w$ at $x=L_x$. We set $E=\beta_w B$ at the right boundary, so that magnetic flux escapes with the bulk flow speed at L_x.

Initially, the incoming stream bounces off the right-hand moving wall of the computational grid. A well defined shock forms as the reflected stream encounters the incoming stream. The shock propagates back to the left toward the injection wall, leaving a hot plasma behind. We have studied shocks for the cases $\sigma=13.3$, 1, and 0.1.

We expect, from the structure of reflected particle solitons, that the $\sigma\geq 1$ results should show a single, well defined Larmor loop of magnetically reflected particles at the front of the shock structure, while the $\sigma=0.1$ calculation should show a more chaotic structure.[11] Momentum conservation requires the peak field amplitude in the layer of reflected particles to be $B_{\max}/B_\infty\approx[1+(2/\sigma)]^{1/2}$. Therefore, when σ is large, the streaming momenta can be absorbed by the magnetic field with a relatively small enhancement above B_∞, so that the $\mathbf{E}\times\mathbf{B}$ drift remains large and the loop is close to a simple cycloid. When $\sigma\ll 1$, the shock jump conditions[3] show that $B_{\max}\gg B_{\text{downstream}}$, the relativistic cyclotron frequency at the peak is $\omega_{c,\text{peak}}\approx\sqrt{2}\omega_p$, the thickness of the peak field region becomes $\sim c/\omega_p$, and the drift velocity near the peak is small, leading to multiple overlapping loops near the field maximum. The dividing line between steady single-loop behavior and unsteady multiple-loop formation occurs at $\sigma\approx 0.2$.

These general expectations are confirmed in our detailed simulations. The phase-space plots in Figs. 1(a)-1(c) show the particles' momenta p_x/mc as a function of x well after the shock separates from the wall. For $\sigma=13.3$ and $\sigma=1$, in Figs. 1(a) and 1(b), a single coherent loop of reflected particles has formed at the leading edge of the shock. For these highly and moderately magnetized cases, the shock velocity is almost constant, and is in accord with the speed expected from the shock jump conditions.[3] The loop structure shows a small oscillation of its amplitude on a time scale of $\simeq$a few$\times mc\gamma_\infty/eB_\infty$. A superluminous precursor in the electromagnetic field is associated with this oscillation.

By contrast, in the weakly magnetized flow ($\sigma=0.1$) the resulting shock structure, shown in Fig. 1(c), is much more scrambled than is the case when $\sigma\geq 1$. Because the overlapping loops are time dependent in the shock frame, the propagation speed is unsteady. However, the average speed remains in good accord with the jump conditions.

The magnetic fields associated with these snapshots of the shock structure are shown in Figs. 2(a)-2(c). The first main peak of the magnetic ramp in the $\sigma=13.3$ and 1 cases [Figs. 2(a) and 2(b)] shows the "double-horned"

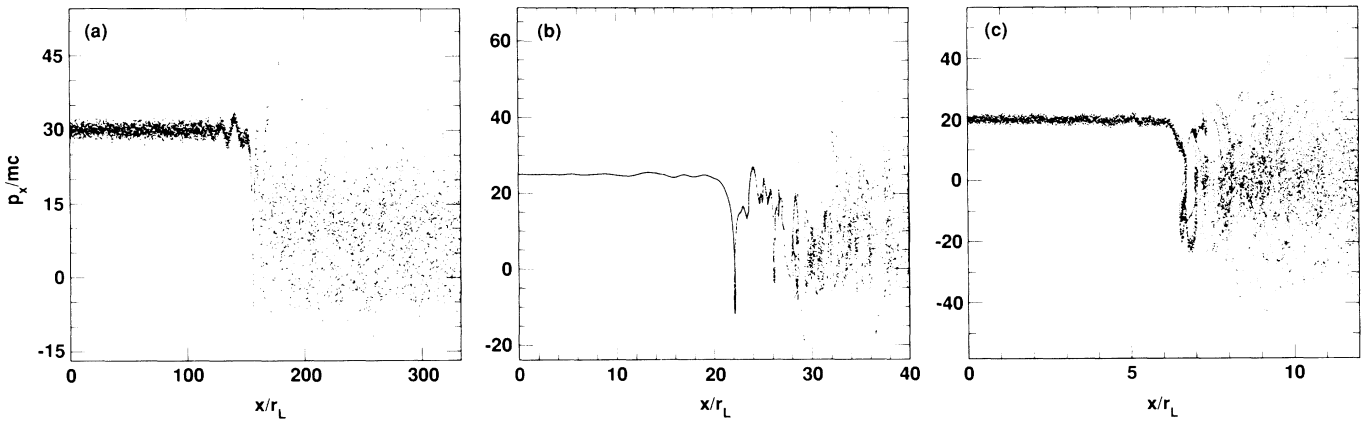

FIG. 1. p_x-x phase space for the three simulations. The Larmor radius r_L is based on the parameters of the upstream flow. (a) Left panel, $\sigma=13.3$. Phase space at $t_{\text{obs}}\approx 250t_c$, where $t_c=mc\gamma_\infty/eB_\infty$, is the cyclotron time based on the upstream flow, with separation time $t_s\approx 70t_c$. The plasma thermalizes in a time $t_{\text{th}}\approx 10t_c$ after the passage of the reflected particle loop in the shock front. (b) Middle panel, $\sigma=1$. Here, $t_{\text{obs}}\approx 44t_c$, $t_s\approx 9t_c$, and $t_{\text{th}}\approx 8t_c$. (c) Right panel, $\sigma=0.1$, with $t_{\text{obs}}\approx 13t_c$, $t_s\approx 8t_c$, and $t_{\text{th}}\approx 3t_c$. When measured relative to the cyclotron time at the magnetic peak of the leading loop of reflected particles, the thermalization time is approximately constant, with $t_{\text{th}}\approx 14t_{c,\text{peak}}$.

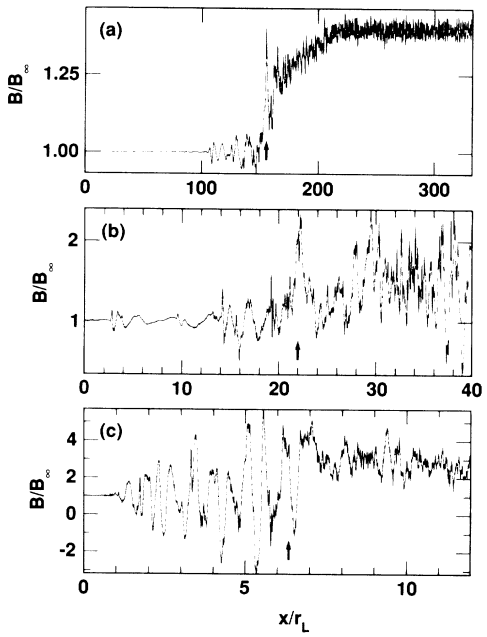

FIG. 2. Magnetic field as a function of position for the three simulations, at the same observation times as in Fig. 1. Note the large magnetic overshoot when $\sigma=0.1$, and the residual magnetic "ramp" left over from the initial conditions in the $\sigma=13.3$ case.

structure characteristic of reflected particle solitons, which arises because the turning points of the cyclotron orbit correspond to infinities in the density of a cold stream.[11] These large particle densities give very large current densities at the two turning points. For small σ, there is a pronounced oscillation of the leading phase-space loop along with a superluminous precursor advancing into the plasma ahead of the main shock, as shown in Fig. 2(c).

After a few looping motions, the unsteady flow looses gyration phase coherence and "thermalizes" by phase mixing downstream of the loop. The downstream distributions have a quasi-Maxwellian form in p_x and p_y. The electromagnetic field still retains a substantial component of the shock's total energy in extraordinary-mode fluctuations. In Table I, we give the fractions of the energy left downstream in the forms of steady fields, rms amplitude of the fluctuating extraordinary modes, and two-dimensional thermal energy, all in the proper frame downstream.

We also give the magnetosonic Mach numbers in the shock frame, and the critical Mach numbers for the existence of magnetosonic solitons: If $M_A < M_1$, there would be flow without reflected particles, while if $M_1 < M_A < M_2 = \sqrt{5}\gamma_\infty$, the soliton contains a single loop of reflected particles. The simulations presented here are of supercritical shocks: Reflection of particles from the shock front plays an essential role in the shock's structure. The structure of the leading loop in our simulations is in accord with that of the soliton theory of Ref. 11.

The mechanism of particle reflection is one prominent difference between these results and simulations of *nonrelativistic* magnetosonic shocks. In nonrelativistic electron-ion shocks, reflected ions forming a large-scale Larmor loop in the shock front have a prominent role in maintaining the magnetic ramp. Reflection, however, depends on the electrostatic field formed because electrons have smaller Larmor radii than the ions. In our strongly relativistic environment, reflection is entirely magnetic.

Another new feature of these relativistic shocks is their ability to thermalize the particle spectra even though spatial variation occurs in only one space dimension. Nonrelativistic, one-dimensional transverse shocks can be sustained by particle reflection, but with the downstream "thermal" pressure replaced by continued coherent Larmor gyration of the ions.[16] Instabilities which transform downstream gyration into heat appear only when spatial variation along **B** is included in the model.[17] In our relativistic simulations, the plasma is thermalized in the plane perpendicular to **B** entirely by processes operating in one dimension; processes analogous to the cyclotron maser instability[18] are promising

TABLE I. Parameters and derived quantities for the shock models. v_w is the flow velocity at the right-hand boundary. v_s is the measured shock speed. The Mach numbers M_A, M_1, and M_2 are discussed in the text. U_{fl}, U_{steady}, and U_{plasma} are the energy densities of the extraordinary-mode fluctuations, the steady fields, and the thermal energy of the plasma, all measured in the proper frame of the downstream plasma. The energy density of bulk flow is negligible; $U_{total}=U_{fl}+U_{steady}+U_{plasma}$. B_{peak} is the maximum amplitude of the magnetic field associated with the leading Larmor loop. There is a discrepancy between the measured and predicted values of B_{peak}/B_∞ in the $\sigma=13.3$ run because the flow has not "forgotten" the initial profile of the magnetic field as a function of position in the plasma filling the box at $t=0$.

σ	γ_∞	v_w/c	v_s/c	M_A	M_1	M_2	$\frac{U_{fl}}{U_{total}}$	$\frac{U_{steady}}{U_{total}}$	$\frac{U_{plasma}}{U_{total}}$	$\frac{B_{peak}}{B_\infty}$	$(1+2/\sigma)^{1/2}$
13.3	30	0.5	0.8	24.3	13.4	199	2×10^{-4}	0.975	0.024	1.4	1.1
1	25	0.5	0.5	43.3	9.4	97	0.03	0.72	0.25	1.7	1.7
0.1	20	0	$\sim$0.45	154	9.9	109	0.12	0.51	0.37	4.6	4.6

candidates for the thermalization mechanism.

Within the limited simulation time for the shock to cross our grid, we have *not* observed the formation of a suprathermal distribution of particle momenta downstream. However, as is clear from Table I, while the plasma has relaxed to an approximately Maxwellian distribution in two velocity dimensions, the downstream state still includes substantial nonthermal power in waves when σ is small. Therefore, it is possible that in plasma-dominated shocks, a significant suprathermal tail may form on time scales long compared with the Larmor time, through resonant and nonresonant interaction between waves and particles in the downstream region.

We conclude from the simulations presented here ($0.1 \leq \sigma \leq 13.3$) that relativistic, collisionless transverse shocks exist and are steady, in electron-positron plasmas. The shock transition is dominated by coherent Larmor-loop structure in the cold flow, accompanied by a spike in the self-consistent magnetic field. Particle heating begins only after the cold flow has traversed the leading loop structure. Significant energy is left in the form of downstream and upstream electromagnetic fluctuations.

The research of two of us (A.B.L. and C.E.M.) was supported by U.S. Department of Energy Contract No. W-7405-ENG-48 to the Lawrence Livermore National Laboratory. That of the other author (J.A.) was supported in part by Grant No. AST-8615816 from the National Science Foundation and by Grant No. 88-11 from the Institute of Geophysics and Planetary Physics at the Lawrence Livermore National Laboratory, both to the University of California at Berkeley.

---

[a]Also at Departments of Astronomy and of Physics, University of California at Berkeley, Berkeley, CA 94720.

[1]For reviews of the role of electron-positron pairs in pulsars, see J. Arons, Space Sci. Rev. **24**, 437 (1979), and in *Positron-Electron Pairs in Astrophysics,* edited by M. Burns, A. K. Harding, and R. Ramaty (American Institute of Physics, New York, 1983), p. 163; M. Salvati and F. Pacini, in *The Origin and Evolution of Neutron Stars,* edited by D. J. Helfand and J.-H. Huang (Reidel, Dordrecht, 1987), p. 79.

[2]J. Piddington, Aust. J. Phys. **10**, 530 (1957); M. J. Rees and J. E. Gunn, Mon. Not. Roy. Astron. Soc. **167**, 1 (1974).

[3]C. F. Kennel and F. V. Coroniti, Astrophys. J. **283**, 694, 710 (1984).

[4]D. J. Helfand and R. H. Becker, Astrophys. J. **314**, 203 (1987).

[5]M. C. Begelman, R. D. Blandford, and M. J. Rees, Rev. Mod. Phys. **56**, 163 (1984).

[6]A. Lightman, A. Zdziarski, and M. J. Rees, Astrophys. J. Lett. **315**, L113 (1987), and references therein.

[7]D. Lynden-Bell, Nature (London) **223**, 690 (1969); R. V. E. Lovelace, Nature (London) **262**, 649 (1976); R. D. Blandford, Mon. Not. Roy. Astron. Soc. **176**, 465 (1976); R. D. Blandford and R. Znajek, Mon. Not. Roy. Astron. Soc. **179**, 433 (1977); R. McDonald and K. S. Thorne, Mon. Not. Roy. Astron. Soc. **198**, 345 (1982).

[8]R. D. Blandford and C. F. McKee, Mon. Not. Roy. Astron. Soc. **177**, 343 (1977).

[9]D. Kazanas and D. Ellison, Astrophys. J. **304**, 178 (1986); J. Blondin and A. Konigl, Astrophys. J. **323**, 451 (1987).

[10]D. A. Clarke, M. L. Norman, and J. O. Burns, Astrophys. J. Lett. **311**, L63 (1986); D. G. Payne, K. Lind, R. Meier, and R. D. Blandford, to be published.

[11]D. Alsop and J. Arons, Phys. Fluids **31**, 839 (1988).

[12]J. Dreher, Astrophys. J. **230**, 687 (1979).

[13]C. F. Kennel and R. Pellat, J. Plasma Phys. **15**, 335 (1976).

[14]A. B. Langdon and B. F. Lasinski, in *Methods in Computational Physics,* edited by J. Killeen (Wiley, New York, 1976), Vol. 16, p. 327.

[15]C. K. Birdsall and A. B. Langdon, *Plasma Physics via Numerical Simulation* (McGraw-Hill, New York, 1985).

[16]M. M. Leroy, D. Winske, C. C. Goodrich, C. S. Wu, and K. Papadopoulos, J. Geophys. Res. **87**, 5081 (1982).

[17]M. M. Leroy, in *Particle Acceleration Processes, Shockwaves, Nucleosynthesis and Cosmic Rays,* edited by L. Koch-Miramond and M. A. Lee (Pergamon, Oxford, 1984), p. 231.

[18]D. B. Melrose, *Plasma Instabilities in the Laboratory and in Space* (Cambridge Univ. Press, Cambridge, 1986), p. 184.

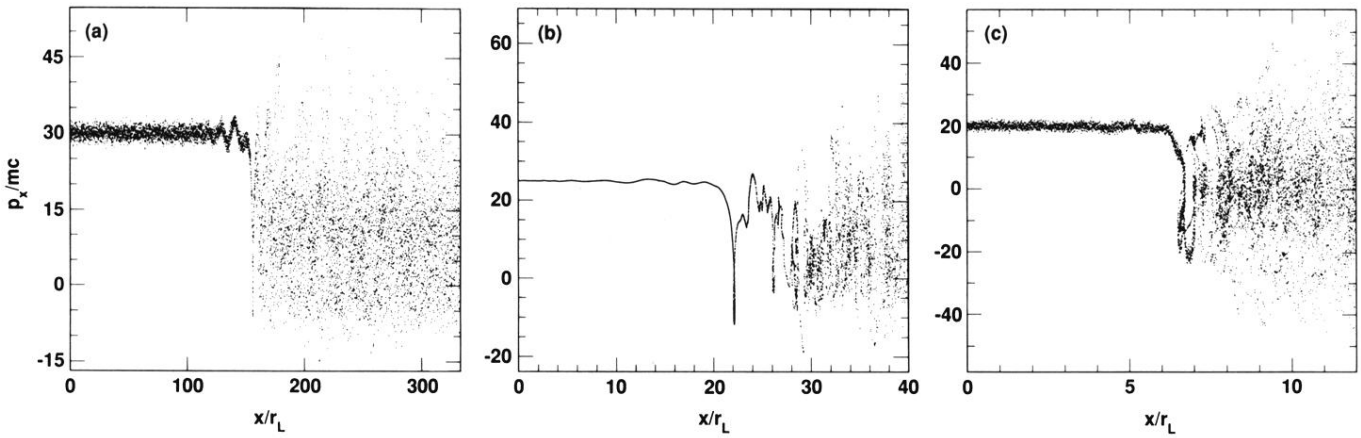

FIG. 1. p_x-x phase space for the three simulations. The Larmor radius r_L is based on the parameters of the upstream flow. (a) Left panel, $\sigma = 13.3$. Phase space at $t_{obs} \approx 250 t_c$, where $t_c = mc\gamma_\infty / eB_\infty$, is the cyclotron time based on the upstream flow, with separation time $t_s \approx 70 t_c$. The plasma thermalizes in a time $t_{th} \approx 10 t_c$ after the passage of the reflected particle loop in the shock front. (b) Middle panel, $\sigma = 1$. Here, $t_{obs} \approx 44 t_c$, $t_s \approx 9 t_c$, and $t_{th} \approx 8 t_c$. (c) Right panel, $\sigma = 0.1$, with $t_{obs} \approx 13 t_c$, $t_s \approx 8 t_c$, and $t_{th} \approx 3 t_c$. When measured relative to the cyclotron time at the magnetic peak of the leading loop of reflected particles, the thermalization time is approximately constant, with $t_{th} \approx 14 t_{c,peak}$.